17

Ultrawideband-over-fiber technologies with directly-modulated semiconductor lasers

Víctor Torres-Company[1], Kamau Prince[2], Xianbin Yu[2],
Timothy Braidwood Gibbon[2] and Idelfonso Tafur Monroy[2]
[1]*Departament de Física, Universitat jaume I*
ES-12071 Castelló, Spain
[1]*Department of Electrical and Computer Engineering, McGill University*
H3A 2A7 Montreal, Canada
[2]*Department of Photonics Engineering, Technical University of Denmark*
DK 2800 Lyngby, Denmark

1. Introduction

In the last few years, there has been a growing interest in the generation of ultrawideband (UWB) radio-frequency (RF) signals. Due to the high-data-rate capabilities, low power consumption and immunity to multi-path fading, these pulses have an unprecedented opportunity to impact radio communication systems in personal area networks, and promise as well substantial applications in radar, safety, and biomedicine. The UWB RF spectrum was regulated between the 3.1 and 10.6 GHz band with a power spectral density of -41.3dBm/MHz, according to the Federal Communications Commission (FCC) of the United States. Later, Asian and also European regulations stated similar masks (Porcine et al., 2003; Di Benedetto et al., 2006). Any signal to be considered as UWB must have an RF spectral bandwidth greater than 500 MHz or a fractional bandwidth greater than 20%. Due to these strict regulations concerning the power levels, UWB systems for wireless communications are constrained to operate over few tens of meters. In addition, this huge spectrum challenges most of the current electronics devices aiming to provide arbitrary waveform generation and simplicity in a single low-cost platform.
However, the synergy between UWB and fiber technologies offers an alternative solution, providing undisrupted service over different networks, while still preserving the high-data-rate capabilities. Moreover, UWB-over-fiber technology opens the possibility to generate the UWB compliant signals directly in the optical domain, thus relaxing the requirements for high-frequency electrical components.
In this Chapter, we review the basic notions of UWB-compliant signals and several widespread all-optical solutions for their generation and distribution. The central core of the Chapter will focus on simple techniques for the generation of doublet and monocycle UWB impulses, particularly those exploiting the dynamics of gain-switched semiconductor laser sources. Finally, we discuss new areas of research in this rapidly evolving field.

2. Review of photonically assisted UWB signal generation

The normalized version (in dB) FCC regulated UWB mask for indoor applications is depicted in Fig. 1 (right column) in dashed line, together with several electrical signals in time and their corresponding RF spectrum. As one can notice, a Gaussian electrical impulse does not satisfy the UWB requirements because it exhibits a high amount of energy at low frequencies. However, monocycle and doublet pulses, corresponding to first- and second-order derivation of Gaussian impulses, start to fit better into the UWB domain. Although they do not strictly fall into the FCC mask, an extra electronic filter could be placed before the transmitting antenna in order to achieve the UWB compliant pulse. Actually, the UWB radiating antenna helps to reduce this low frequency content. Although not a perfect solution, most researchers have focused into the generation of this kind of pulses because of their relative simplicity. A higher-order UWB pulse matches the mask without the need of filtering, but their generation requires more advanced techniques.

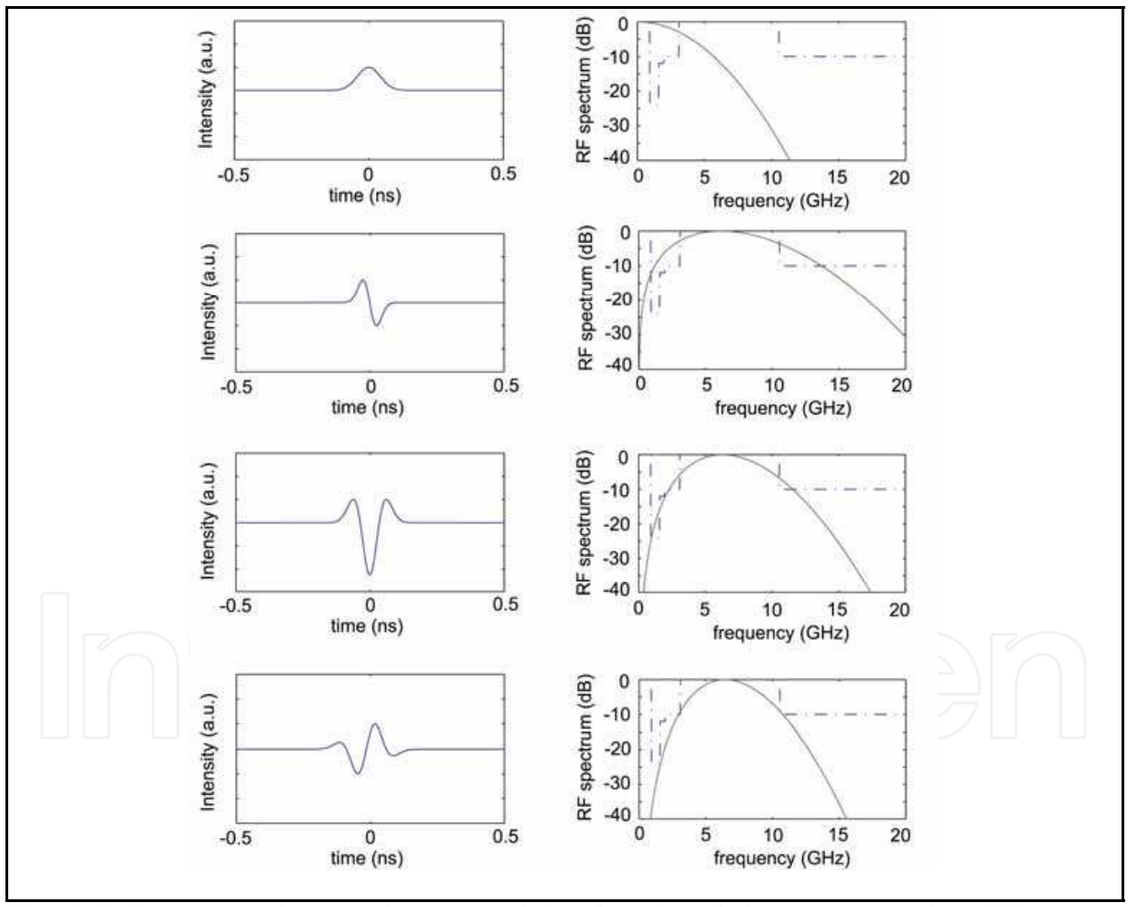

Fig. 1. Different impulse signals in time (left column) and their corresponding RF spectra (right column). The FCC UWB normalized mask is displayed in dashed line.

In this section we aim to review some of the work previously published on optical approaches for UWB signal generation. The list of references does not pretend to be

exhaustive, but it gives a flavour of the research trend in this topic from a historical and intuitive perspective.

2.1 Dispersion-induced frequency-to-time mapping

The first photonic approaches about generation of UWB pulses focused on the technique now known as "frequency-to-time mapping". This solution aims at synthesizing the power spectrum of an ultrashort optical pulse and subsequently launching the signal into a linear dispersive medium. Because each frequency component travels at a different group velocity, after a certain amount of dispersion, the output intensity pulse becomes a scaled replica of the synthesized power spectrum (Fetterman et al. 1979; Tong et al. 1997). The scaling factor is provided by the group-delay-dispersion (GDD) coefficient of the dispersive medium (Muriel et al. 1999). Larger amounts of dispersion do not change the shape of the pulse, only increase the scale. The electrical UWB impulse is subsequently obtained by ideal photodetection. Due to the scaling factor capabilities, this technique for arbitrary waveform generation allows for entering into the low-frequency regime. An added advantage of this technique is that when a single-mode optical fiber is used as the stretching element, the signal is generated and transported in the same optical component without the need for chromatic dispersion compensation.

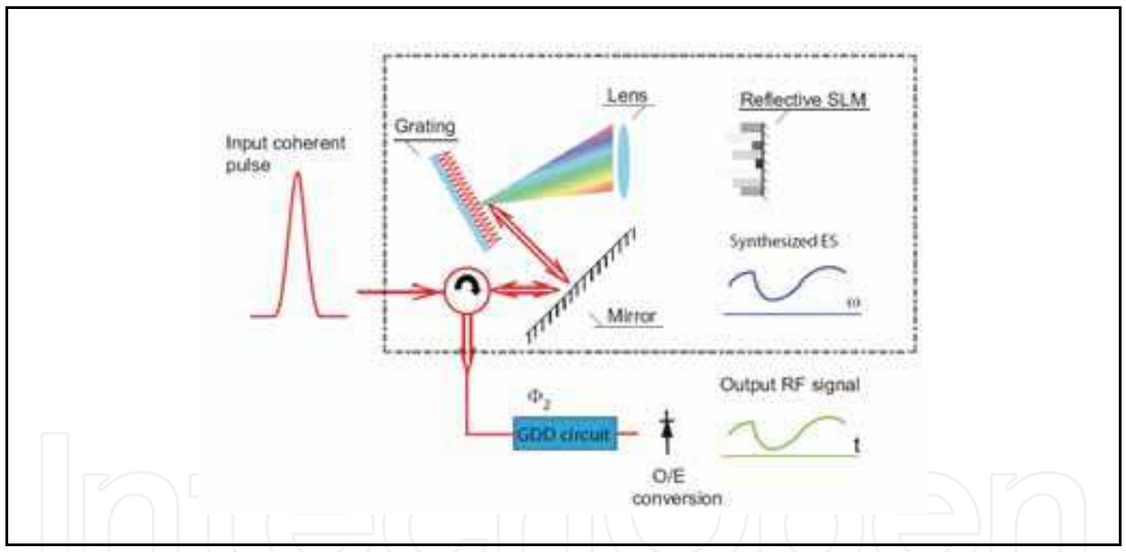

Fig. 2. Example of arbitrary microwave waveform generation based on Fourier transform pulse shaping and dispersion induced frequency-to-time mapping.

The first demonstration used a supercontinuum light source and a Fourier transform pulse shaper for the spectrum synthesizer (Chou et al., 2003). Later on, this technique incorporated a closed loop enabling rapid waveform design thanks to the reconfigurability of the spatial light modulator used in the pulse shaper (Lin et al., 2005). The high flexibility and resolution of this technique allow for the elimination of undesired ripples (apodization) and optimization of the RF spectrum of the signal to satisfy the FCC spectral regulations with a precision better than that offered by monocycle or doublet impulses (McKinney et al. 2006). More recently, fiber filters have been used to replace the Fourier transform shaper device,

leading to a more compact setup, but at the expense of sacrifying the reconfigurability capabilities (Wang et al. 2007). A recent solution deserves a special mention (Abtahi et al., 2008). There, an all-fiber reconfigurable optical filter, together with differential photodetection, permits obtaining Gaussian, monocycle, doublet and higher-order UWB impulses in a single device just by tuning a simple band-pass optical filter.
Although this frequency-to-time mapping technique provides an impressive flexibility in the synthesis of the UWB RF spectrum, the use of a broadband laser pulse as optical source restricts the repetition rate to a few MHz. A recent solution replaces the mode-locked laser by a broadband incoherent light source (Torres-Company et al., 2008). However, in this case, the shaping is performed on the averaged intensity profile, which means that because of the incoherent nature of the approach, there are uncontrolled changes in the pulse to pulse shape (Torres-Company et al., 2007).

2.2 Nonlinear optics

The first alternative approaches to the frequency-to-time mapping made use of the cross-phase modulation effect either in a highly nonlinear fiber (HNLF) (Zeng et al., 2007) or in a semiconductor optical amplifier (SOA) (Dong et al., 2007). The idea behind this is to induce a frequency chirp with a Gaussian pump pulse on a continuous wave (CW) probe laser. This phase modulation can be transformed into intensity modulation by using an appropriate optical band-pass filter. A nice feature of this system is that it permits the control of the polarity of the generated UWB pulse just by tuning the wavelength of the CW to fit in the positive or negative slope region of the optical Gaussian filter. Optimized spectral filters lead to a better control of the shape of the pulse, extending the technique to include doublet impulses too (Zeng et al., 2007). However, the HNLF approach still requires of a high-power laser pulse as pump signal to induce the chirping on the CW probe. On the other hand, the monocycle impulses generated using the SOA approach deviate from the ideal shape due to undesired effects such as the chirping in the dynamics of the process.
A recent approach has demonstrated the generation of generating UWB monocycle impulses with polarity control using sum-frequency generation (SFG) in a periodically-poled lithium niobate waveguide. This system provides a compact device and does not require a femtosecond light source (Wang et al., 2009). Doublet impulses could in principle be generated as well. However, the required power levels to excite SFG in the waveguide are still very high, leading to a low-efficiency global process.

2.3 Microwave photonic filtering design

Microwave photonics is nowadays a well-established research field. In general terms, it aims to provide processing functions of RF and microwave signals that are difficult to achieve using purely electronic approaches (Capmany and Novak, 2007). One of the most widely explored aspects of microwave photonics is radio-frequency filtering (Capmany et al., 2005). The advantages offered by photonics are reconfigurability, high bandwidth, immunity to electromagnetic interference, high-speed processing, and potential integrability with fiber optics technology. In a photonic microwave filter, the input RF signal modulates an optical source, the modulated optical waveform is then processed in a photonic circuit, and finally the signal is recovered back in the electrical domain by optoelectronic (O/E) conversion (Capmany et al., 2005). In the former approaches, filtering functions were implemented

using "positive" taps only, which implies that the filter is always pass-band at low frequencies. This drawback may be solved, e.g., by employing alternative modulation formats combined with differential photodetection, or nonlinear effects in either SOAs or SMFs (You and Minasian, 2004; Minasian, 2004; Capmany et al., 2005).
It has been recently recognized that monocycle impulses can be generated by filtering a Gaussian electrical impulse in a two-tap (one positive and another negative) microwave photonic filter; whereas doublet impulses are obtained in a three-tap configuration (two-positives and another negative and vice versa) (Yao, 2007). This general rule permits to recover the previous research work on incoherent filter design with positive and negative taps for the particular problem of UWB signal generation. Microwave photonic filters featuring reconfigurability are the preferred ones because they provide extra control on the UWB generated signal. In addition, since many of the synthesized filters require the use of a single-mode-fiber to achieve the required delays, the system generates and transports the signal simultaneously.

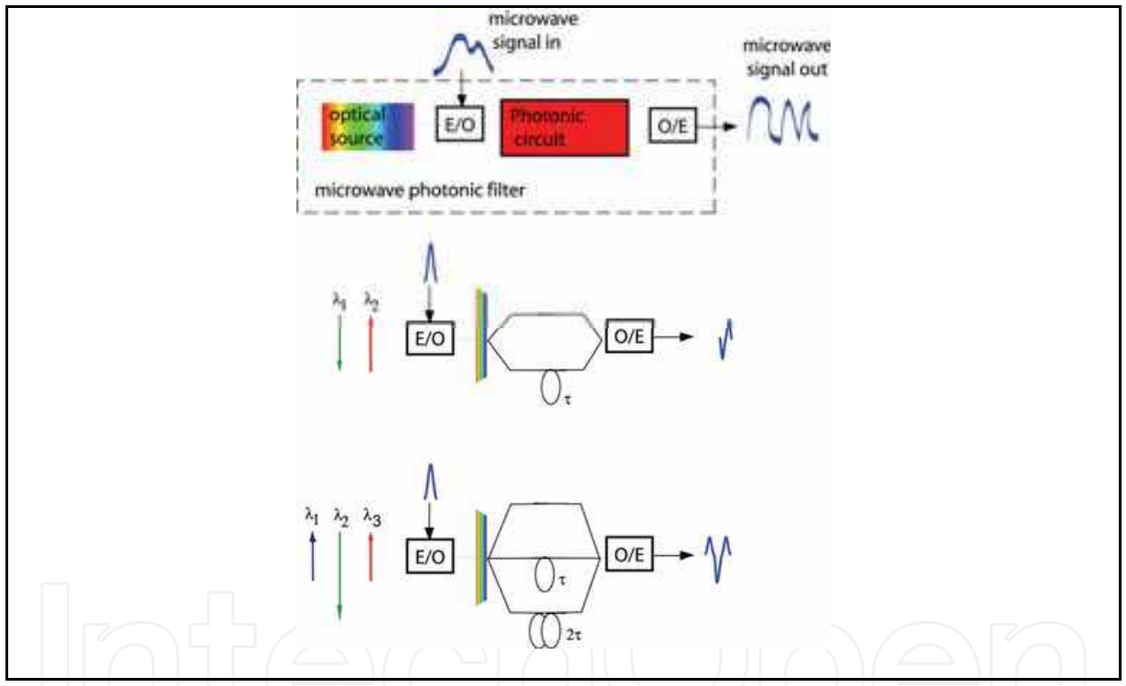

Fig. 3. General concept of a microwave photonic filter. Scheme for the generation of a monocycle and doublet with a microwave photonic filter with positive and negative taps.

For example, we mention the generation of monocycle and doublet impulses based on cross-gain modulation (XGM) in an SOA (Wang et al., 2006). XGM was one of the first approaches that recognized the capabilities to generate negative taps in a microwave photonic filter (Coppinger et al., 1997). Other approaches include the use of a polarization modulator and birefringent fibers (Yao & Wang, 2007) or the bias dependence with the wavelength in an electro-optic modulator (Li et al., 2008; Vidal et al. 2005). A very recent approach (Bolea et al., 2009) deals with the performance of an N-tap microwave photonic filter implemented with two EOMs and several switches (Capmany et al. 2003). Although the performance of

this microwave filter is more complex than the previous setups, the reconfiguration capabilities and the possibilities to implement alternative modulation schemes to ON-OFF keying makes the system very promising for UWB-over-fiber technologies.

3. UWB signal generation based on semiconductor laser dynamics

In this section we report an alternative photonic technique to generate UWB pulses. It involves the use of a distributed feedback (DFB) laser whose driving current is modulated by an electrical data signal (Torres-Company et al., 2008b; Torres-Company et al., 2008c). With respect to previous approaches, our configuration offers an efficient solution in terms of power consumption and constitutes a low-cost alternative, since there are no optical nonlinear processes involved requiring extra light sources or additional active optical devices. Our approach requires a single optical light source and avoids the use of external electro-optic modulation. It is worth mentioning that a previous reported work (Lin & Chen, 2006) used a current modulated Fabry-Perot laser for the generation of UWB signals. However, unlike in our approach, the frequency chirp was not used for achieving UWB signal generation. Instead, monocycle pulses were obtained by O/E conversion and subsequent differentiation performed in the electrical domain.

With our setup, monocycle or doublet pulse shapes can be achieved. Although the experimental arrangement is the same in both cases, the physical mechanism behind is different. The general setup consists on a DFB semiconductor laser, a 12.5 Gb/s bit pattern generator, and a spectral pass-band optical filter. The DFB laser is nominally specified for operation at 10 Gb/s, but the driving data signal was selected at the maximum bit rate. The output pulse from the laser is spectrally filtered by the band- pass filter, which had a Gaussian profile and a FWHM of 0.3 nm. The way of selecting the UWB-pulse shape is by adjusting the bias voltage applied to the laser, the amplitude of the data driving signal and the tunable filter. There are two sets of parameters that lead to either monocycle or doublet shapes. We now proceed to formulate a heuristic explanation for each of the different physical phenomenon behind this achievement.

3.1 Monocycle generation using the chirping effect

In this case, the laser is forward biased far from the threshold, and a relatively low value of modulating amplitude is selected. The laser dynamics is found in the linear region of the Power–Intensity curve. The key is that, as a result of the changes in the carrier population, the refractive index also changes, leading to a phase-modulation changing with time (Agrawal, 2002). Therefore, in the small-signal case the laser pulse becomes highly chirped, with an instantaneous frequency resembling the shape of a monocycle. Then, as heuristically explained in Fig. 4, the process of chirp-to-intensity conversion can be achieved by using a spectrally linear optical filter. This behavior is obtained approximately by placing our Gaussian bandpass filter at the linear slope region.

Of course, this is just a heuristic explanation and instantaneous frequencies do not always exist in the spectrum of a coherent signal (Mandel, 1974). Even more, the case displayed in Fig. 4 is only valid for phase-only modulated signals. However, let us formulate mathematically our problem. The complex field of the frequency-chirped pulse is filtered by a linear optical filter $H(\omega) = A(\omega + \omega_s)$, where A is a real constant that determines the slope of

the filter and ω_s denotes the vertical offset from the zero-crossing point. The temporal envelope at the output of the filter is given by

$$\psi_{out}(t) = i\,A\,[\psi_{in}(t) - i\,\omega_s\psi_{in}(t)] \tag{1}$$

where the prime denotes temporal derivation and $\psi_{in}(t)$ is the input temporal envelope. We have taken into account that $FT^{-1}[-i\,\omega\Psi_{in}(\omega)] = \psi_{in}(t)$, where $\Psi_{in}(\omega) = FT[\psi_{in}(t)]$, with FT and FT^{-1} denoting Fourier and inverse Fourier transformation, respectively. We can always rewrite the input envelope as $\psi_{in}(t) = I^{1/2}_{in}(t)\exp[-i\varphi_{in}(t)]$, where $\varphi_{in}(t)$ and $I_{in}(t)$ denote the phase and normalized intensity modulation, respectively. We now assume that the frequency modulation dominates respect to the intensity modulation, but its contribution value is less than the corresponding frequency offset of the filter, i.e., $|I_{in}'(t)| << |\varphi_{in}'(t)| << \omega_s$. With this assumption, and after some algebra, the optical intensity at the output of the filter can be approximated to

$$I_{out}(t) \approx 2\,A^2\,\omega_s\,I_{in}(t)\,[\varphi_{in}'(t) + \omega_s/2]\,. \tag{2}$$

The above equation establishes that the light intensity at the output of the optical filter is given essentially by the frequency chirp of the input optical pulse if the intensity profile is relatively smooth. The derivation of Eq. (2) accounts for the heuristic explanation provided in Fig. 4.

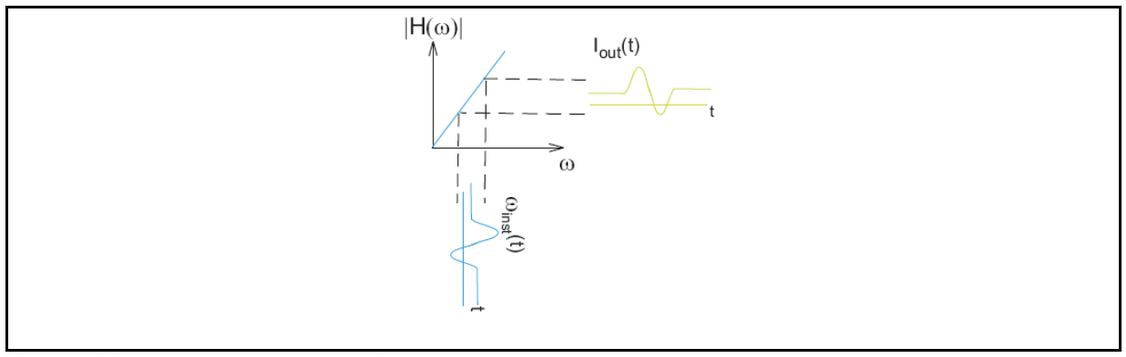

Fig. 4. Schematic overview of chirp-to-intensity conversion.

To test this approach we have built the setup corresponding to Fig. 5. The laser was biased at 67 mA, a value far from the threshold of 30 mA, and the bit pattern generator produced a sequence of one ”1” followed by seven ”0” with a peak-to-peak voltage of 0.57 V. The measured intensity and chirp are displayed at Fig. 6(a) in solid and dashed line, respectively. For the measurement of the chirp we employed the transport-of-intensity equation procedure (Dorrer, 2005), for which an SMF of 0.415km was used. We can appreciate the monocycle-like profile of the chirp. The spectrum corresponding to the laser and the filter, when located at the optimal point to achieve the monocycle shape, are displayed together in Fig. 6(b). The average optical power level before and after the filter was measured to be 5.6dBm and −9.1dBm, respectively.

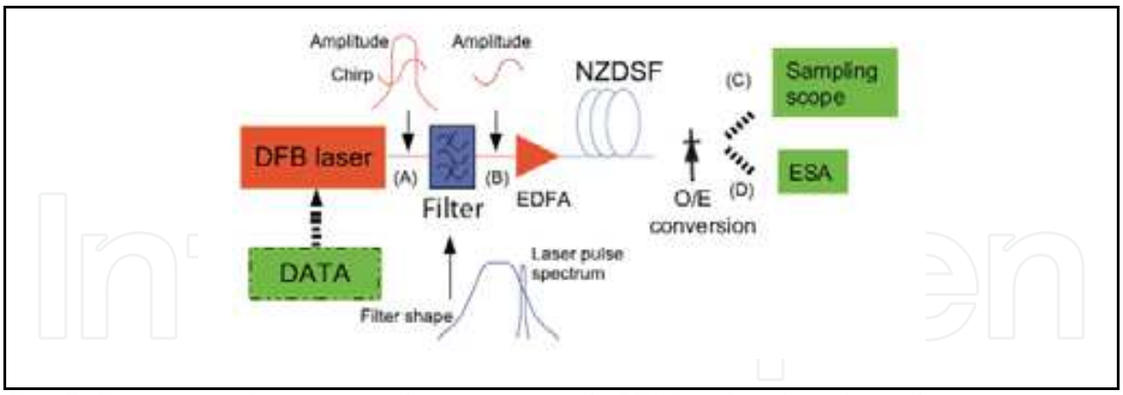

Fig. 5. Experimental setup to achieve monocycle UWB pulses based on chirp-to-intensity conversion.

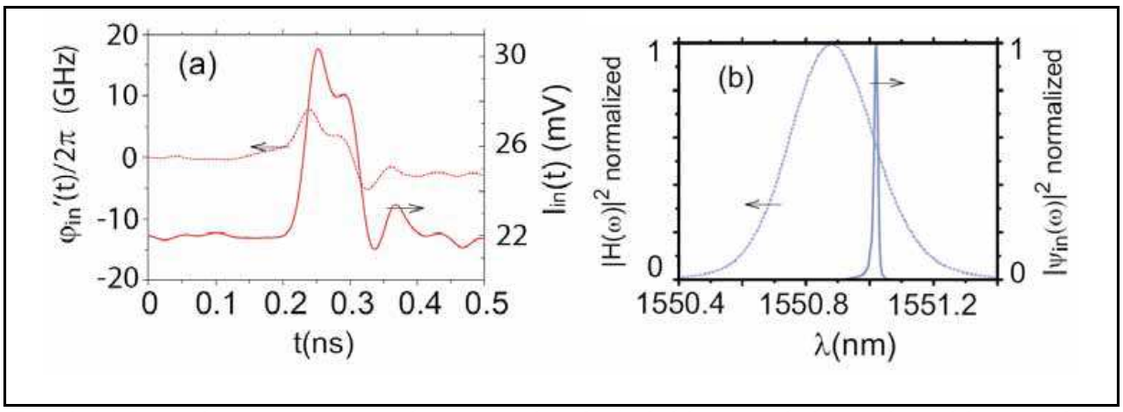

Fig. 6. (a) Input laser intensity pulse in amplitude (solid line) and chirp (dotted line) and (b) normalized spectrum of laser pulse (solid line) and amplitude filter (dotted line).

In order to test the validity of the signal for UWB communications we performed an additional transmission experiment. The optical signal is amplified by an Erbium-doped fiber amplifier (EDFA) and propagated through 20 km of non-zero dispersion shifted fiber (NZDSF) with 4.5dB loss and 5 ps/nm/km dispersion. This dispersion leads to a GDD parameter very low to distort the achieved UWB pulse. The intensity waveform at the output is detected by a 10GHz bandwidth photodiode (PD) which intrinsically assists in smoothing undesired high-frequency RF components that do not fall into the UWB range. The resultant electrical signal is measured in the RF domain by an electrical spectrum analyzer (ESA) with a resolution of 1MHz, and in the time domain by a sampling oscilloscope. The EDFA is adjusted so that the receiver gets an average optical input power of −0.5 dBm. Figure 7 shows the measured resultant UWB signal consisting of a monocycle-like pulse in time and frequency domain. For the frequency domain picture, we selected a repetition rate of 390.6MHz (a ”1” followed by 32 ”0”) so that the achieved spectral shape is properly sampled. As it can be appreciated, the RF spectrum spreads over the UWB region. Due to the monocycle-like waveform, non-disregarding low-frequency content still remains, which can be minimized by reducing the power into the photodiode with some extra attenuator.

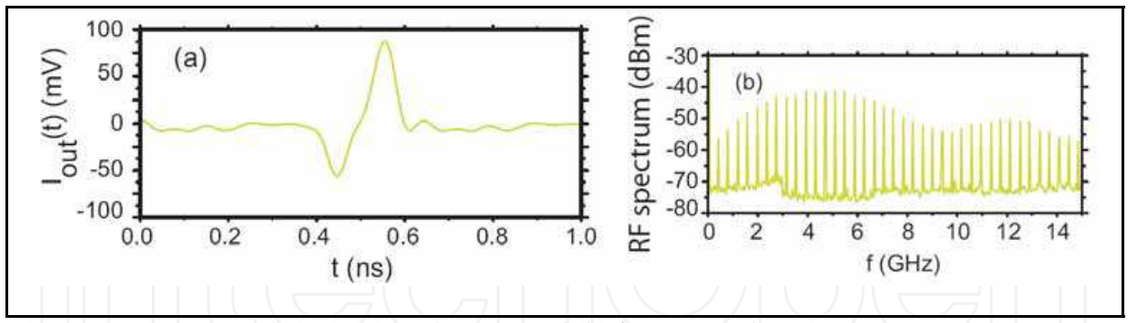

Fig. 7. UWB monocycle in (a) time domain and (b) frequency domain.

3.2 Overshooting effect

Using the same components we can also achieve a doublet UWB pulse. The physical principle behind is showed in Fig. 8 (a). We drive the DFB laser with the electrical inverted data from the pattern generator, and forward bias it with a current close to the threshold (at 35mA in the experiments). In the large-signal modulation regime, the laser power overshoots at the rising edge due to relaxation oscillations and then reaches the steady state (Agrawal, 2002). We can then filter this radiation with an optical filter in order to reshape the waveform to achieve the desired doublet UWB profile.

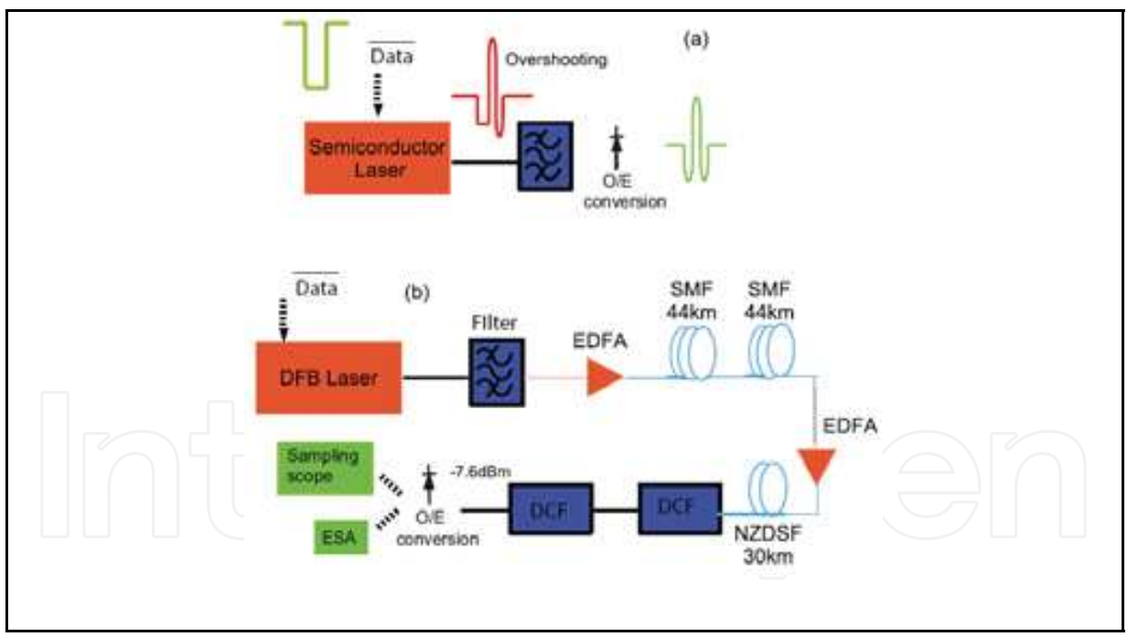

Fig. 8. (a) Heuristic explanation of the physical principle to achieve the UWB doublet. (b) Experimental setup.

Figure 9(a) shows the electrical data pulse (green dash-dotted line) applied to the laser, and the output optical intensity (red solid line). The overshooting effect at the trailing edge of the pulse is apparent. The power oscillates at the relaxation oscillation frequency before achieving a steady state following the shape of the driving electrical signal. We measured

the RF spectrum of this waveform with the 10 GHz bandwidth PD and verified that it was not UWB compliant. However, we were able to produce the required pulse characteristics by passing this laser pulse through the same Gaussian spectral filter as before, but at a different operation point. In Fig. 9(b) we show the output laser spectrum (blue solid line) and the filter profile placed in the optimal position to achieve the doublet shape. As we can see, the high-frequency optical components are smoothed. It should be mentioned that previously-reported approaches for optical filtering of gain-switched lasers tried to avoid this overshooting effect and aimed to generate bellshaped ultrashort waveforms (Nakazawa et al. 1990; Niemi et al. 2001). Our goal here is instead to optimize the intensity profile so that this waveform can be exploited for UWB RF signal generation. After the optical filtering, we converted the optical signal into the electrical domain with a 10 GHz bandwidth PD, and succeeded in generating a doublet-like UWB impulse, as shown by the green line in Fig. 10 (a).

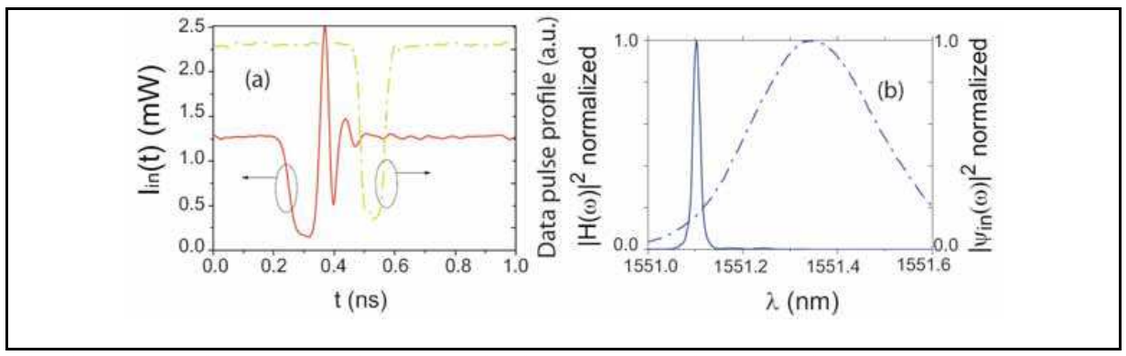

Fig. 9. (a) Intensity laser profile (red solid line) and electrical data signal (green dashed line). The temporal scale has a different origin for the electrical and optical signals. (b) Normalized spectrum of laser pulse (solid line) and amplitude filter (dotted line).

In order to verify the usefulness of this method we performed an additional experiment for propagating the signal through an optical fiber link. For this evaluation, the signal needed to be amplified after optical filtering and the O/E converter was placed at the receiver. As indicated in Fig. 8(b), the fiber link is comprised of two stages. We first propagated the signal through two SMF coils of 44km length each. Then the optical signal was further amplified and propagated through 30 km of NZDSF as well as 13km of DCF, matched to compensate for the dispersion introduced by the SMF in the first stage. This constitutes a total optical link length of 118 km, which represents the largest distance ever reported for UWB signal distribution, to the best of our knowledge. The output optical pulse is detected with the 10GHz bandwidth photodiode and measured simultaneously in the time domain with a sampling oscilloscope, and in frequency domain with an ESA with 1MHz measurement resolution. The achieved signal is displayed in Figs. 10(b) and (c). It possesses a central frequency of 7 GHz and has a 10 dB bandwidth of 10.2 GHz, hence a fractional bandwidth of 146 %. The pulse duration was measured to be 236 ps. Comparison of Figs. 10(a) and (b) indicates that there is no significant distortion of the UWB pulse during propagation. The spikes in Fig. 10c are due to the fact that we introduced a data sequence of one ”1” followed by sixteen ”0”, so that the RF spectrum of a single UWB pulse is conveniently sampled at 0.78 GHz for illustration purposes. We achieved higher data

transmission rates with this optical pulse shape, up to a soft limit related to the output UWB pulse duration. We have successfully transmitted similar pulses at 3.12 GHz over this fiber link.

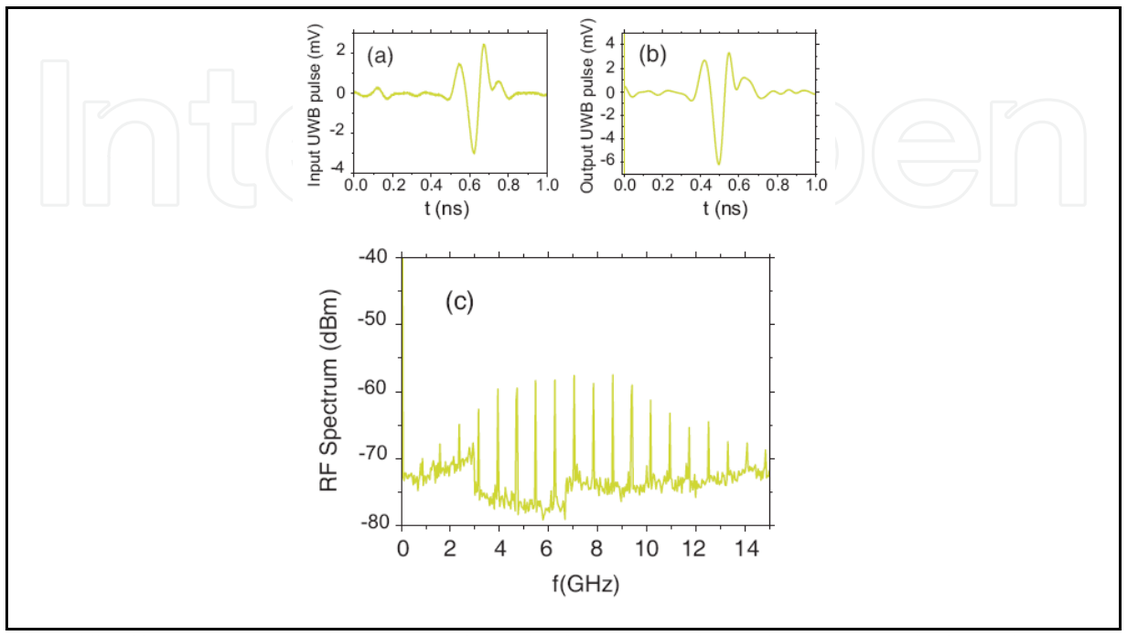

Fig. 10. Generated UWB doublet in (a) time domain before transmission; (b) after propagation in the 118 km fiber link and (c) spectral domain.

4. Current trends in photonically assisted UWB-over-fiber

4.1 Advanced modulation formats

Most of the discussion carried out through the Chapter has dealt with the generation of direct sequence (DS) UWB impulses assuming an ON-OFF keying modulation format. However, different modulation schemes such as pulse-position-modulation, pulse-polarity modulation, orthogonal pulse modulation or amplitude pulse modulation are being investigated. For instance, DS code division multiple access (DS-CDMA) is a widespread technique in multiple-user wireless communications. In this direction, several photonic approaches for bi-phase coded UWB impulse generation exist. We mention, for example, the use of phase-to-amplitude conversion in multichannel fiber gratings (Dai and Yao, 2008); a spectral filter in a Sagnac loop (Li et al., 2007); or polarization modulation (Ou et al., 2008). A recent solution based on a higher-order multi-tap reconfigurable microwave photonic filter features most of the previous modulation formats in a single platform (Bolea et al., 2009).

Another approach worth mentioning is the generation of direct-sequence binary phase shift keying (DS-BPSK) modulated UWB signals based on the overshooting effect in a distributed feedback (DFB) laser (Yu et al., 2009). The experimental setup is shown in Fig. 11. A continuous wave (CW) laser modulated by a 12.5 Gb/s Mach-Zenhder modulator (MZM) is injected into the first-order lasing side mode of a DFB laser biased close to the threshold. As a consequence of this, the DFB laser experiences cross-gain modulation along with associated overshooting relaxation oscillations. The effect is similar to that described in

section 3.2, the difference being that the DFB laser is not directly modulated, but instead undergoes indirect optical cross-gain modulation. No optical pulse shaper is required, making this UWB generation technique particularly simple and attractive.

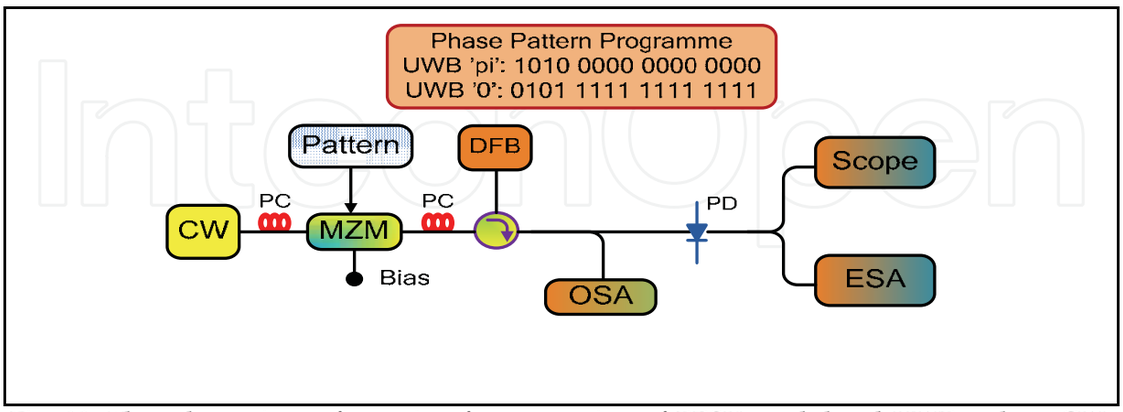

Fig. 11. The schematic configuration for generation of BPSK modulated UWB pulses. CW: continuous-wave laser, MZM: Mach-Zenhder modulator, PC: polarization controller, DFB: distributed feedback laser, OSA: optical spectrum analyzer, PD: photodiode, ESA: electrical spectrum analyzer.

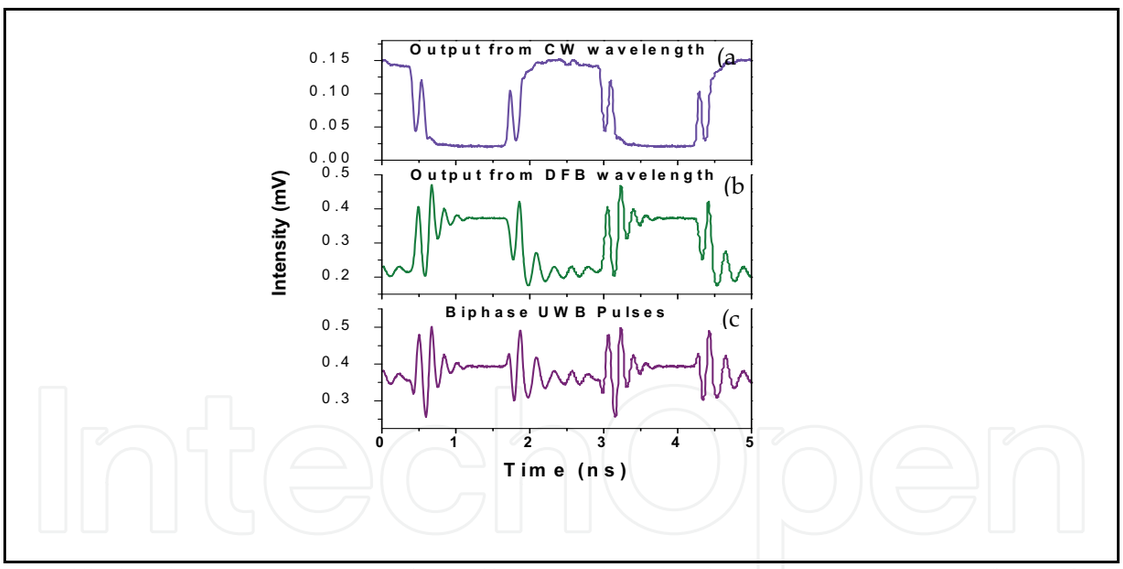

Fig. 12. (a) the output pattern from CW wavelength, (b) the output pattern from DFB wavelength, (c) the calculated biphase UWB pulses from summation of (a) and (b).

At the output of the circulator an UWB pulse is formed from the incoherent summation of the CW and DFB wavelengths. This is shown in Fig. 12, where Fig. 12(a) is the measured output pattern from CW wavelength, (b) is the measured output pattern from DFB wavelength, and (c) is the calculated biphase UWB pulses calculated from the summation of the measured signals of (a) and (b). Assuming the phase of the pulse generated by the 12.5 Gbit/s pattern '1010 0000 0000 0000' in is π, and the phase of the pulse generated by

pattern '0101 1111 1111 1111' is 0, then it is evident from that binary phase shift keying coded pulses are generated.
Figure 13 shows the experimentally generated 781.25 Mb/s UWB signals in the time and frequency domains for the bit sequence 0 π 0 π. The electrical spectrum shows good compliance with the FCC mask. Use of externally injected DFB lasers is not limited to the generation of DS-BPSK UWB signals and has also been used for OOK UWB signals as well (Gibbon et al., 2009) .

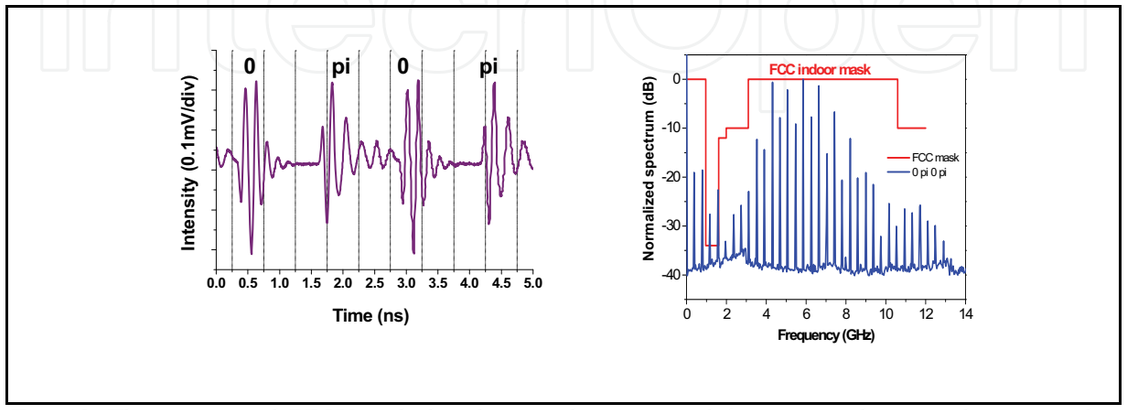

Fig. 13. The generated BPSK coded pulses in the time and frequency domains by using the pattern sequence 0 π 0 π.

4.2 UWB pulse shapes "on demand" and antenna distortion compensation

UWB is a wireless communication technology. Most of the previous approaches for photonic generation of UWB impulses assume that the photodetected signal is going to be transferred into the antenna without any significant degradation. However, as recently realized by several groups, this is not the case (McKinney et al., 2008; Abtahi et al., 2008b). The reason is that most UWB antennas do not have a perfect flat response into the UWB region specified by the FCC regulations. Besides, the wireless transmission and the receiver antenna also introduce appreciable changes in the phase and amplitude of the spectrum of the UWB signal. Therefore, the pulse measured at the photodiode is usually significantly different to the one measured at the receiver, thus limiting the range, speed and capabilities of the technology. However, most of these distortions are linear and can be compensated for by synthesizing a predistorted pulse (McKinney and Weiner, 2006; Abtahi et al., 2008b) or by post-compensating the pulse (Hamidi and Weiner, 2009), so that the received signal is a truly UWB impulse waveform.
To this aim, optical pulse shaping technology using either spatial light modulators or fiber Bragg gratings and the frequency-to-time mapping effect has been employed. This constitutes an excellent example of the capabilities of photonic approaches to overcome some of the problems that current electronics-based technology suffers.

4.3 Range extension of high bit rate UWB signals

The users' increasing demands on broadband and seamless services require that cellular voice and multimedia services are always available everywhere. Therefore, a system high bit

rate and long reach distance is highly desired for next generation networks to meet this requirement. In this case, the generation of high speed UWB signals and its range extension become more and more attractive. However, the communication range of UWB technology is limited due to the FCC mask and emission power level constraints. This becomes more critical as the data rate increases. Basically, the higher the data rate, the lower is the range. This provides a big challenge. Recently, a 500Mb/s UWB signal transmission over 65cm wireless distance has been demonstrated (Abtahi et al., 2008b), and a research group in Singapore demonstrated an experiment with 500 Mbps data rate wireless UWB transmission over 4m in 2003 (Peng et al., 2005).
Digital signal processing (DSP) technology has the well-known advantages of good noise tolerance, high sensitivity and high flexibility. DSP based receivers are expected to improve the wireless propagation performance and subsequently extend the range, which is an important feature to further enhance the usefulness of UWB based high-rate products.

5. Conclusions

UWB-over-fiber is an emerging research field offering an increased range of operation for this high-rate wireless technology. We have focused on simple photonic solutions based on semiconductor laser dynamics to generate UWB electrical impulses. In particular, we have demonstrated that monocycle and doublet impulses can be generated based on the chirping and overshooting effects, respectively. As basic equipment, we have used directly modulated laser and optical band-pass filtering with a Gaussian spectral profile. Although our approach constitutes a very simple solution, the price to pay is the low flexibility in the design of the pulse shape and the absence of reconfigurability capabilities. We have pointed out alternative solutions that feature different modulation formats and shapes, as well as reviewed some exciting possibilities enabled by photonic approaches.

6. Acknowledgments

This work has been partially funded by the Spanish Ministry of Science and Innovation (MCINN, research project FIS2007-62217) and the Convenio Universitat Jaume I-Fundació Caixa Castelló (project P1 1B2007-09). Victor Torres acknowledges the MCINN and Spanish Foundation for Science and Technology for a postdoctoral Fellowship. Timothy Gibbon acknowledges the Villum Kann Rasmussen Fonden for a postdoctoral Grant.

7. References

Abtahi M.; Mirshafiei M.; Magné J.; Rusch L. A. & LaRochelle S. (2008). Ultra-wideband waveform generator based on optical pulse shaping and FBG tuning. *IEEE Photon. Technol. Lett.*, Vol. 20, No. 2, 135-137.

Abtahi M.; Mirshafiei M.; LaRochelle S. & Rusch L. A. (2008). All-optical 500Mb/s UWB transceiver: an experimental demonstration. *J. Lightwave Technol.*, Vol. 26, No. 13, 2795-2802.

Agrawal G. P. (2002). *Fiber-Optics Communication Systems,* John Wiley & sons, New York.

Bolea M.; Mora J.; Ortega B. & Capmany J. (2009). Optical UWB pulse generator using an N tap microwave photonic filter and phase inversion adaptable to different pulse modulation formats. *Opt. Express*, Vol. 17, No. 7, 5023-5032.

Capmany J.; Pastor D.; Martínez A.; Ortega B. & Sales S. (2003). Microwave photonic filters with negative coefficients based on phase inversion in an electro-optic modulator. *Opt. Lett.*, Vol. 28, No. 16, 1415-1417.

Capmany J. & Novak D. (2007). Microwave photonics combines two worlds. *Nature Photon.*, Vol. 1, No. 6, 319-330.

Capmany J.; Ortega B.; Pastor D. & Sales S. (2005). Discrete-time optical processing of microwave signals. *J. Lightwave Technol.*, Vol. 23, No. 2, 702-723.

Chou J.; Han Y. & Jalali B. (2003). Adaptive RF- photonic arbitrary waveform generator. *IEEE Photon. Technol. Lett.*, Vol. 15, No. 4, 581-583.

Coppinger F.; Yegnanarayanan S.; Trinh P. D. & Jalali B. (1997). All-optical incoherent negative taps for photonic signal processing. *Electron. Lett.*, Vol. 33, No. 11, 973-975.

Dai Y. & Yao J. P. (2008). Optical generation of binary phase-coded direct-sequence UWB signals using a multichannel chirped fiber Bragg grating. *J. Lightwave Technol.*, Vol. 26, No. 15, 2513-2520.

Di Benedetto M. -G.; Kaiser T.; Molish A. F.; Oppermann I. & Politano, C. (2006). *UWB Communication Systems: A Comprehensive Overview,* Hindawi Publishing, ISBN, New York.

Dong J; Zhang X; Xu J.; Huang D.; Fu S. & Shum P. (2007). Ultrawideband monocycle generation using cross-phase modulation in a semiconductor optical amplifier. *Opt. Lett.*, Vol. 32, No. 10, 1223-1225.

Dorrer C. (2005). Characterization of nonlinear phase shifts by use of the transport-of-intensity equation. *Opt. Lett.*, Vol. 30, No. 23, 3237-3239.

Fetterman H. R.; Tannenwald P. E.; Parker C. D.; Melngailis J. & Williamson R. C. (1979). Real-time spectral analysis of far-infrared laser pulses using a SAW dispersive delay line. *Appl Phys. Lett.*, Vol. 34, No. 2, 123-125.

Gibbon T. B.; Yu X; Zibar D. & Tafur Monroy I. (2009). Novel ultra-wideband photonic signal generation and transmission featuring digital signal processing bit error rate measurements. *OFC/NFOEC2009 Conference Proceedings*, California, USA, Paper: OTuB8.

Hamidi E & Weiner A. M. (2009). Post-compensation of ultra-wideband antenna dispersion using microwave photonic phase filters and its applications to UWB systems. *IEEE Trans. Microw. Theory Techn.*, Vol. 57, No. 4, 890-898.

Li J.; Xu K.; Fu S.; Wu J.; Lin J.; Tang M. & Shum P. (2007). Ultra-wideband pulse generation with flexible pulse shape and polarity control using a Sagnac interferometer-based intensity modulator. *Opt. Express*, Vol. 15, No. 26, 18156-18161.

Li J.; Fu S.; Xu K.; Lin J.; Tang M. & Shum P. (2008). Photonic ultrawideband monocycle pulse generation using a single electro-optic modulator. *Opt. Lett.*, Vol. 33, No. 3, 288-290.

Lin I. S.; McKinney J. D. & Weiner A. M. (2005). Photonic synthesis of broadband microwave arbitrary waveforms applicable to ultra-wideband communication. *IEEE Microw. Wireless Compon. Lett.*, Vol. 15, No. 4, 226-228.

Lin W. P. & Chen Y. C. (2006). Design of a new optical impulse radio system for ultra-wideband wireless communications. *IEEE J. Sel. Top. Quantum Electron.,* Vol. 12, No. 4, 882-887.

Mandel L. (1974). Interpretation of instantaneous frequencies. *Am. J. Phys.*, Vol. 42, No. 10, 840-846.

McKinney J. D. & Weiner A. M. (2006). Compensation of the effects of antenna dispersion on UWB waveforms via optical pulse-shaping techniques. *IEEE Trans. Microw. Theory Techn.*, Vol. 54, No. 4, 1681-1682.

McKinney J. D.; Lin I. S. & Weiner A. M. (2006). Shaping the power spectrum of ultra-wideband radio-frequency signals. *IEEE Trans. Microw. Theory Techn.*, Vol. 54, No. 12, 4247-4255.

McKinney J. D.; Peroulis D. & Weiner A. M. (2008). Time-domain measurements of the frequency delay of broadband antennas. *IEEE Trans. Ant. Prop.*, Vol. 56, No. 1, 39-47.

Minasian R. A. (2006). Photonic signal processing of microwave signals. *IEEE Trans. Microw. Theory Techn.*, Vol. 54, No. 2, 832-846.

Muriel M. A.; Azaña J. & Carballar A. (1999). Real-time Fourier transformer based on fiber Braga gratings. *Opt. Lett.,* Vol. 24, No. 1, 1-3.

Nakazawa M.; Suzuki K. & Kimura Y. (1990). Transform-limited pulse generation in the gigahertz region from a gain-switched distributed-feedback laser diode using spectral windowing. *Opt. Lett.,* Vol. 15, No. 12, 715-717.

Niemi T.; Zhang J. G. & Ludvigsen H. (2001). Effect of filtering on pulses generated with a gain-switched DFB laser. *Opt. Commun.,* Vol. 192, No. 3, 339-345.

Ou P.; Zhang Y. & Zhang C.-H. (2008). Optical generation of binary phase-coded direct-sequence ultra-wideband signals by polarization modulation and FBG-based multi-channel frequency discriminator. *Opt Express,* Vol. 16, No. 7, 5130-5135.

Peng X.; Png K. B.; Srivastava V. & Chin F. (2005) High Rate UWB Transmission with Range Extension, IEEE ICU 2005, Switzerland, (Invited paper).

Porcine D.; Research P. & Hirt W. (2003). Ultra-wideband radio technology: potential and challenges ahead. *IEEE Commun. Mag.,*Vol. 41, No. 7, 66-74.

Tong Y. C.; Chan L. Y. & Tsang H. K. (1997) Fiber dispersion or pulse spectrum measurement using a sampling oscilloscope. *Electron. Lett.* Vol. 33, No. 11, 823-825.

Torres-Company V.; Lancis J. & Andrés P. (2007) Incoherent frequency-to-time mapping: application to incoherent pulse shaping. *J. Opt. Soc. Am. A.* Vol. 24, No. 3, 888-894.

Torres-Company V.; Lancis J.; Andrés P. & Chen L. R. (2008) Reconfigurable RF-waveform generation based on incoherent filter design. *J. Lightwave Technol.* Vol. 26, No. 15, 2476-2483.

Torres-Company V.; Prince K. & Monroy I. T. (2008b) Fiber transmission and generation of ultrawideband pulses by direct current modulation in semiconductor lasers and chirp-to-intensity conversion. *Opt. Lett.* Vol. 33, No. 3, 222-224.

Torres-Company V.; Prince K. & Monroy I. T. (2008c) Ultrawideband pulse generation based on overshooting effect in gain-switched semiconductor laser. *IEEE Photon. Technol. Lett.* Vol. 20, No. 13, 1299-1301.

Vidal B.; Corral J. L. & Martí J. (2005) All-optical WDM microwave filter with negative coefficients. *IEEE Photon. Technol. Lett.* Vol. 17, No. 3, 666-668.

Wang Q.; Zeng F.; Blais S. & Yao J. P. (2006) Optical UWB monocycle pulse generation based on cross-gain modulation in a semiconductor optical amplifier. *Opt. Lett.* Vol. 31, No. 21, 3083-3086.

Wang C.; Zeng F. & Yao J. P. (2007) All-fiber ultrawideband pulse generation based on spectral shaping and dispersion-induced frequency-to-time mapping. *IEEE Photon. Technol. Lett.* Vol. 19, No. 3, 137-139.

Wang J.; Sun Q.; Sun J. & Zhang W. (2009) All-optical UWB pulse generation using sum-frequency generation in a PPLN waveguide. *Opt. Express* Vol. 17, No. 5, 3521-3530.

Yao J. P. (2007) Photonic generation of ultrawideband signals. *J. Lightwave Technol.* Vol. 25, No. 11, 3219-3235.

Yao J. P. & Wang Q. (2007) Photonic microwave bandpass filter with negative coefficients using a polarization modulator. *IEEE Photon. Technol. Lett.* Vol. 19, No. 9, 644-646.

You N. S. & Minasian R. A. (2004) All-optical photonic signal processors with negative coefficients. *J. Lightwave Technol.* Vol. 22, No. 12, 2739-2742.

Yu X; Gibbon T. B.; Zibar D. & Tafur Monroy I. (2009). A novel incoherent scheme for photonic generation of biphase modulated UWB signals. *OFC/NFOEC2009 Conference Proceedings*, California, USA, Paper: JWA60.

Zeng F.; Wang Q. & Yao J. P. (2007) All-optical UWB impulse generation based on cross-phase modulation and frequency discrimination. *Electron. Lett.* Vol. 43, No. 2, 121-122.

IntechOpen

Optical Fiber New Developments
Edited by Christophe Lethien

ISBN 978-953-7619-50-3
Hard cover, 586 pages
Publisher InTech
Published online 01, December, 2009
Published in print edition December, 2009

The optical fibre technology is one of the hop topics developed in the beginning of the 21th century and could substantially benefit applications dealing with lighting, sensing and communication systems. Many improvements have been made in the past years to reduce the fibre attenuation and to improve the fibre performance. Nowadays, new applications have been developed over the scientific community and this book fits this paradigm. It summarizes the current status of know-how in optical fibre applications and represents a further source of information dealing with two main topics: the development of fibre optics sensors, and the application of optical fibre for telecommunication systems.

How to reference
In order to correctly reference this scholarly work, feel free to copy and paste the following:

Víctor Torres-Company, Kamau Prince, Xianbin Yu, Timothy Braidwood Gibbon and Idelfonso Tafur Monroy (2009). Ultrawideband-over-Fiber Technologies with Directly-Modulated Semiconductor Lasers, Optical Fiber New Developments, Christophe Lethien (Ed.), ISBN: 978-953-7619-50-3, InTech, Available from: http://www.intechopen.com/books/optical-fiber-new-developments/ultrawideband-over-fiber-technologies-with-directly-modulated-semiconductor-lasers

INTECH
open science | open minds

InTech Europe
University Campus STeP Ri
Slavka Krautzeka 83/A
51000 Rijeka, Croatia
Phone: +385 (51) 770 447
Fax: +385 (51) 686 166
www.intechopen.com

InTech China
Unit 405, Office Block, Hotel Equatorial Shanghai
No.65, Yan An Road (West), Shanghai, 200040, China
中国上海市延安西路65号上海国际贵都大饭店办公楼405单元
Phone: +86-21-62489820
Fax: +86-21-62489821

IntechOpen